Freeze-Drying of Aqueous Solution Frozen with Prebuilt Pores

Wei Wang
School of Chemical Machinery, State Key Laboratory of Fine Chemicals, Dalian University of Technology, Dalian 116024, China

College of Life Science, Dalian Nationalities University, Dalian 116600, China

Dapeng Hu
School of Chemical Machinery, State Key Laboratory of Fine Chemicals, Dalian University of Technology, Dalian 116024, China

Yanqiu Pan and Yanqiang Zhao
School of Chemical Engineering, State Key Laboratory of Fine Chemicals, Dalian University of Technology, Dalian 116024, China

Guohua Chen
Dept. of Chemical and Biomolecular Engineering, The Hong Kong University of Science and Technology, Hong Kong, China

School of Environmental and Biological Science and Technology, Dalian University of Technology, Dalian 116024, China

College of Life Science, Dalian Nationalities University, Dalian 116600, China

DOI 10.1002/aic.14769
Published online March 11, 2015 in Wiley Online Library (wileyonlinelibrary.com)

To save drying time and increase productivity, a novel idea was proposed for freeze-drying of liquid materials by creating an initially unsaturated frozen structure. An experimental investigation was carried out aiming at verifying the idea using a multifunctional freeze-drying apparatus. Mannitol was selected as the primary solute in aqueous solution. Liquid nitrogen ice-cream making method was used to prepare the frozen materials with different initial porosities. Results show that freeze-drying can be significantly enhanced with the initially unsaturated frozen material, and substantial drying time can be saved compared with conventional freeze-drying of the initially saturated one. Drying time was found to decrease with the decrease in the initial saturation. The drying time for the initially unsaturated frozen sample ($S_0 = 0.28$ or 0.69 of initial porosity) can be at best 32% shorter than that required for the saturated one ($S_0 = 1.00$ or zero porosity). This unique technique is easy to implement and improves the freeze-drying performance of liquid materials. © 2015 American Institute of Chemical Engineers *AIChE J*, 61: 2048–2057, 2015
Keywords: freeze-drying, liquid material, unsaturated, initial saturation, prebuilt pore

Introduction

Freeze-drying has the advantages of protection against chemical decomposition, minimum loss of activity, good preservation of solid structure, and easy rehydration of product due to the low drying temperature and the normally very low residual moisture content.[1] Freeze-drying, therefore, plays an irreplaceable role in the processing of heat-sensitive materials such as food, pharmaceuticals, and biological products.[2,3] It has also found applications in the preparation of new materials.[4] However, freeze-drying is one of the most energy-consuming unit operations because not only of the phase change of moisture but also of the poor overall energy efficiency of the process.[5,6] Reducing freeze-drying time so as to reduce the energy consumption and raise productivity has thus been a worldwide challenge for the past several decades.[7,8]

There are a few ways on the process development to minimize drying time while maintaining acceptable product quality. The ordinary or conventional method involved reducing the chamber pressure in an attempt to improve the driving force of mass transfer. Ultralow vacuum pressure, however, resulted in a very poor thermal conductivity of the dried layer and yielded a large heterogeneity in heat transfer.[9] Light gas injection (e.g., He, H_2) and pulsed pressure in the drying chamber were then tested to improve the conductivity,[10] but this remedy is unlikely to be cost-effective and causes additional operating complexity. In fact, a simple way from the viewpoint of energy saving is that freeze-drying should be carried out at the highest possible temperature, which is limited by the so-called "maximum allowable temperature." This temperature indicates the "eutectic

Correspondence concerning this article should be addressed to G. Chen at kechengh@ust.hk or W. Wang at dwwang@dlut.edu.cn

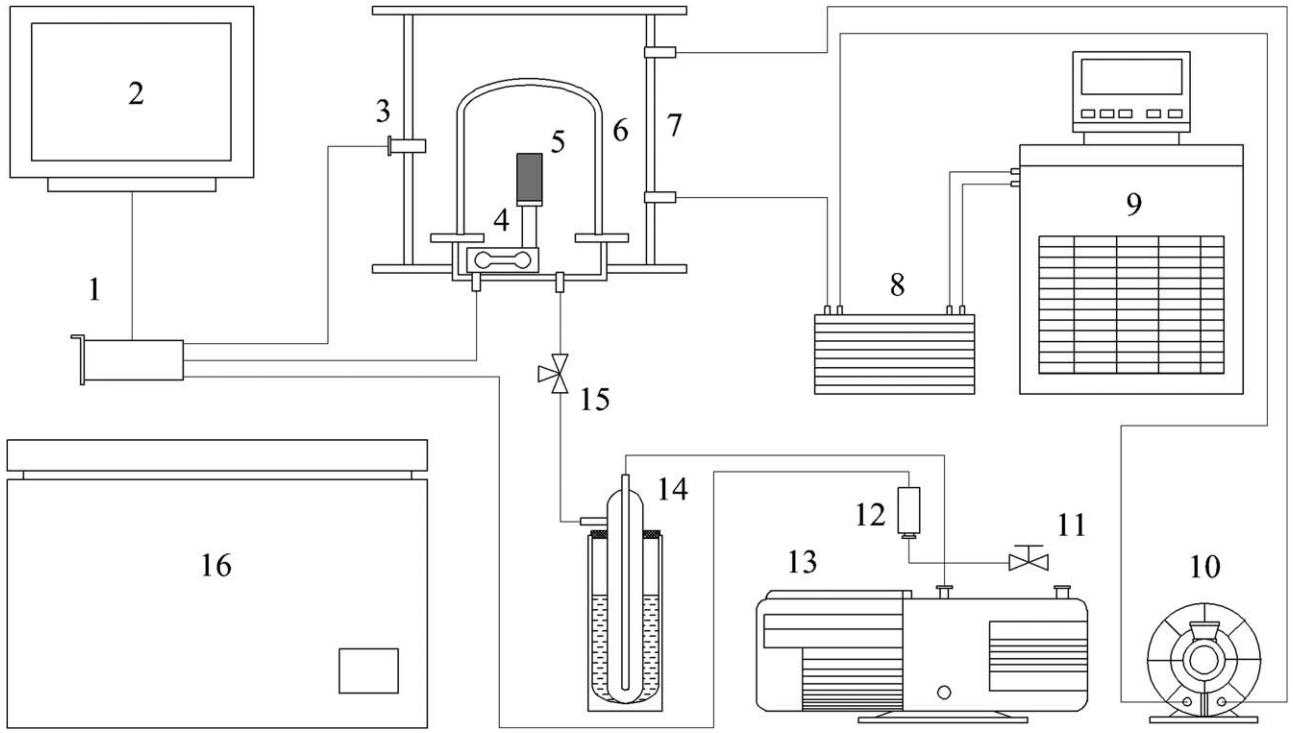

Figure 1. Flow diagram of experimental apparatus: (1) date acquisition card; (2) PC; (3) infrared sensor; (4) loadcell; (5) sample mold; (6) drying chamber; (7) heating cabinet; (8) heat exchanger; (9) circulator; (10) ring blower; (11) regulating valve; (12) pressure sensor; (13) vacuum pump; (14) cool trap; (15) three-way valve; and (16) freezer.

temperature" for a solute that crystallizes during freezing, or the "glass transition temperature" for a solute that remains amorphous.[11] An alternative and effective approach to enhancing the process was to apply volumetric heating, for example, microwave or radio frequency heating. Microwave heating is recognized to be an advanced heating method in contrast to the poor heat supply in conventional freeze-drying conducted and/or radiated from the exterior to the interior of the material being dried. Characteristics of microwave heating can be beneficial in the drying of materials containing liquid water through the volumetric dissipation of dielectric energy. Because ice, unlike water, hardly absorbs microwave energy, simple combination of freeze-drying with microwave heating is ineffective. Wang and Chen, therefore, proposed the "freeze-drying with dielectric-material-assisted microwave heating." Their experimental and numerical results show that using the dielectric material in microwave freeze-drying can effectively improve the freeze-drying rate. More than 20% of the drying time can be saved compared with the conventional process under the examined operating conditions.[12,13]

The dielectric-material-assisted microwave freeze-drying successfully solved the heat-transfer problem in freeze-drying. In terms of mass transfer, there are still certain problems to be addressed. The overall freeze-drying process involves four usual operations, that is, wet material freezing, vacuum maintenance, sublimation–desorption, and vapor condensation. The sublimation–desorption consumes nearly half of the overall energy required. Both the vacuum maintenance and the vapor condensation require similar amounts of energy. The remaining 4–5% of the energy consumption is spent in the freezing stage.[14] As a result, reducing sublimation–desorption time, while simultaneously shortening the vacuum maintenance and vapor condensation times, plays a critical role in the process enhancement and economic improvement. Mass transfer is essential in this part of the process.

Conventional freeze-drying of aqueous solutions is to freeze liquids into a block of frozen materials without any initial voids, termed initially "saturated" frozen material. Sublimation, especially during the primary drying stage, takes place only at the sublimation interface[15] that is more or less the cross-sectional area of the material-containing vial.[16] Conversely, some naturally formed solid materials like meat, vegetables, and fruits have their original porous microstructures. Such materials may initially be "unsaturated," that is, only partially filled with moisture. The sublimation interface in such cases can then be all over the material volume with a much larger surface area.[17,18] In their investigation of the effect of chamber pressure on heat and mass transfer during freeze-drying, Livesey and Rowe found that the rate-controlling factor in the initial stage is heat transfer, but that mass transfer comes to dominate once a dried layer has formed.[19] Mass transfer plays a more important role in the overall freeze-drying process. Wolff and coworkers proposed that water vapor diffusivity in the porous-dried layer is the major factor affecting the drying rate based on their experimental data collected from vial freeze-drying of milk.[20] Nail and Gatlin agreed that the greatest resistance to vapor transport is located at the dried region,[21] depending on the size of the ice crystals formed during the freezing stage.[22] Wang and Chen reached a similar conclusion based on their theoretical analyses of freeze-drying.[23] Pikal and coworkers more specifically pointed out that the prevailing transfer resistance in freeze-drying is from water vapor migration in the dried region.[9,24]

To reduce the drying time and increase the energy utilization efficiency, a novel idea, freeze-drying of an initially unsaturated porous frozen material, was proposed, aiming at improving the mass transfer.[25] The unique feature of this innovation is that the solution to be dried is first prepared into a frozen material with a certain initial porosity (like ice-cream), and then freeze-dried. This technique is expected to yield better product quality and faster drying rate with easy operation. In a preliminary experimental study, two samples, initially saturated and unsaturated ones with the same sample mass of 1.2 g, of the same height–diameter ratio and the same initial moisture content, were tested under the same operating conditions. The initially unsaturated frozen material was dried more than 30% faster.[26] This result verified the previously reported theoretical prediction.[18] The main objective of this study is to further verify the proposed idea through more precise experiments under various operating conditions. The results obtained can help ones to elucidate the mechanism of the process improvement in-depth so as to guide future implementation of the proposed process. This new technique would have a significant impact on the traditional freeze-drying process.

Experimental Apparatus

The laboratory-scale multifunctional experimental apparatus of freeze-drying was designed and built as shown in Figure 1. The apparatus consists of four subsystems: a vacuum system, a temperature control system, a data acquisition system, and a freezing system. It is briefly summarized below.

The vacuum system consists of a drying chamber, a vacuum pump, and a vapor condenser. A quartz bell jar (TGP) was used as the drying chamber with about 2.3 L of volume. A vacuum pump (RV12, BOC Edwards, UK) was operated to maintain an ambient pressure level within the drying chamber under the control of a regulating valve (Swagelok). The vapor condenser is a home-designed liquid nitrogen cool trap with a volume of about 1.7 L to prevent water vapor from entering the pump. This system could develop a vacuum of less than 1 Pa in the drying chamber within 2 min when all the connections were completely sealed.

The temperature control system was designed to maintain a constant ambient temperature on the surface of the bell jar. It includes a circulator, a copper–zinc brazed plate heat exchanger, a ring blower, and a heating cabinet. The circulator (9712, PolyScience) has a wide temperature range from -40 to 200°C and a high stability of ± 0.01°C of the set point. The air–water heat exchanger (Yalong, Jiangsu, China) has an area of 0.72 m^2, and an operating temperature range between -160 and 200°C. The blower (Sensen, Zhejiang, China) has a flow rate of 60 m^3/h and a pressure head of 11.8 kPa for air circulation. The heating cabinet was homemade of plexiglass.

The data acquisition system is comprised of three sensors, a data acquisition card, and a PC (M7130, Lenovo, China). An infrared sensor (CI3A, Reytek) was chosen to monitor the surface temperature of the bell jar. A loadcell (0.3 kg, NTS, Xiamen, China) was mounted to measure the sample's weight loss with time during drying. The loadcell was calibrated against an analytical balance (PL403, Mettler, Switzerland). The vacuum pressure sensor used in the system is an active Pirani gauge (APG100-XLC, BOC Edwards, UK). The data acquisition card (PCI-6221, NI) digitizes the analog signals generated by the three sensors. A computer program was written based on the LabVIEW software platform for data display, storage, and analysis.

The freezing unit is an ultralow temperature freezer (148 L, Aucma, China) outside the drying chamber. It was used for further freezing of the ice-cream-like frozen materials for hardening.

Materials and Facilities

Mannitol (Analytical Grade, Aladdin, China) was selected as the primary solute in aqueous solution because it is a commonly used pharmaceutical excipient which can retain a porous structure and reduce the chance of collapse during and after freeze-drying.[2,27] Deionized water was used as the solvent. Liquid nitrogen was purchased from the Dalian Institute of Chemical Physics of the Chinese Academy of Sciences.

A draught drying cabinet (DHG-9070A, Yiheng, China), a moisture analyzer (HR83-P, Mettler, Switzerland), and a scanning electronic microscope (SEM) (Quanta450, FEI) were also used.

Experimental Method

Sample preparation

The aqueous solution of mannitol was prepared by dissolving 20 g of mannitol powder and 2.3 g of an emulsion stabilizer with 100 g of deionized water in a beaker of 250 mL. The emulsion stabilizer was a mixture of 2.0 g of skim milk powder and 0.3 g of sodium carboxymethylcellulose (CMC). The skim milk is a typical emulsifier, and the CMC is widely used as an emulsifier in food processing.[28] The initial moisture content, X_0, was 4.48 kg/kg on a dry basis, corresponding to 81.77 wt % on a wet basis.

The liquid nitrogen ice-cream making method was used in this experiment instead of the traditional method to prepare the frozen material with a certain initial porosity. A traditional ice-cream making process usually includes mixing, homogenizing, ripening, initial freezing, and further freezing.[29] During the first stage of freezing, a certain amount of air needs to be mixed into the material through agitation as a separate step.[30] The liquid nitrogen ice-cream making method incorporates the initial freezing with gas mixing into one step. This method was adopted because it is convenient for laboratory experimentation. The unsaturated frozen material made with this instant method is expected to have continuous solid matrix and pore space as seen in the following section.

The liquid nitrogen was added slowly into the aqueous solution in an insulated barrel while stirring at about 400 rpm. Gasification of the liquid nitrogen absorbed a large amount of heat resulting in quick freezing of the solution. At the same time, a certain amount of nitrogen gas was incorporated into the solution through the rapid agitation. The solution being processed thus expanded into a frozen mousse with an initial porosity which depended on the amount of liquid nitrogen added with good operational skills. Such a premade material was then molded in several cylindrical containers with supporting pad at bottom, and quickly placed into the freezer for further freezing and hardening for at least 4 h to reach -26°C. The molding allowed forming the samples of equal mass. The molding and hardening operations were almost the same as the further freezing stage in the traditional ice-cream making method.[29] Thereafter, the

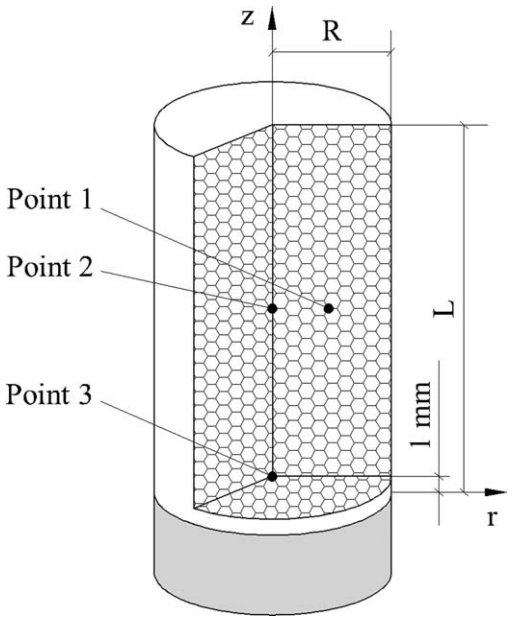

Figure 2. Sample mold.

completely frozen material was fixed onto the supporting pads to form several sample molds within the containers.

For the saturated frozen materials without initial pores, the molds were prepared by directly pouring the aqueous solution into the cylindrical containers and placed into the freezer until they reached −26°C, the preset temperature.

Four kinds of the sample molds, one for the initially saturated frozen material and the others for the unsaturated ones with different initial porosities, were prepared with the same initial mass of 1.8 g and the geometry of 14.8 mm in diameter, as shown in Figure 2.

The initial sample mass, W_0 (kg), was obtained by weighing the sample using the analytical balance. The solid volume, V_s (m^3), of the frozen sample can thus be obtained with the following formula

$$V_s = \frac{1}{1+X_0} \cdot \frac{W_0}{\rho_s} \tag{1}$$

where ρ_s (kg/m^3) is the solid density.[13] With the two volumes, V_0 (m^3) of the initially saturated sample and V'_0 (m^3) of the initially unsaturated one, the initial saturation, S_0, and the intrinsic porosity, ε, of the sample can then be determined, respectively, as

$$S_0 = \frac{V_0 - V_s}{V'_0 - V_s} \tag{2}$$

$$\varepsilon = \frac{X_0 \rho_s}{X_0 \rho_s + S_0 \rho_i} \tag{3}$$

where ρ_i (kg/m^3) is the density of pure ice.[13]

It should be mentioned that when the frozen sample is fully saturated with ice crystals without initial pores, the saturation value is equal to 1. When the sample has initial voids, the saturation value is less than 1. For example, the sample with the initial saturation, S_0 of 0.28 has the intrinsic porosity, ε of 0.96 (when all moisture is removed) and the initial porosity, $\varepsilon(1\text{-}S_0)$ of 0.69 (when no moisture is removed). Table 1 gives these values for the three kinds of the initially unsaturated frozen samples and those for the saturated one.

Table 1. Values of S_0, ε, and $\varepsilon(1\text{-}S_0)$ of Different Frozen Samples

S_0	ε	$\varepsilon(1\text{-}S_0)$
1.00	0.88	0
0.65	0.92	0.32
0.43	0.94	0.54
0.28	0.96	0.69

To investigate temperature evolutions inside the samples during drying, three thermocouples were buried inside two samples, one for the unsaturated frozen sample with the initial saturation of 0.28 as a representative and the other for the saturated one, at different locations. As shown in Figure 2, the sample dimension is supposed to be L in height and R in radius with $z = 0$ at the top surface of the pad. Test points 1, 2, and 3 were, respectively, located at (r, z) of ($R/2$, $L/2$), (0, $L/2$), and (0, 1 mm).

Experimental procedures

Before freeze-drying, the contained sample mold was first moved out of the freezer temporarily to remove the container. This was achieved by allowing it to stand at room temperature for a while or holding it in hand for a moment. The mold without the container was then placed back into the freezer for about 30 min to ensure a uniform initial temperature. Thus, the well prepared sample mold was ready to be freeze-dried.

To avoid an undesirable increase in sample temperature prior to the start of the experiments, the sample mold was moved into the drying chamber as quickly as possible, and the chamber was evacuated immediately. The heat needed for drying came solely from radiation of the quartz bell jar toward the sample surface, and the jar surface was at the ambient temperature of the drying chamber. The data acquisition system displayed and recorded the sample mass, W_t (kg), the ambient temperature and the ambient pressure automatically at a given frequency.

The detailed experimental procedures were executed as follows:

1. Turn on the circulator (9 in Figure 1, the same below) and the blower (10) to preheat the drying chamber (6) to the desired temperature. Check the cool trap (14) to make sure that liquid nitrogen is being supplied.

2. Switch off the regulating valve (11) and adjust the three-way valve (15) to connect the drying chamber to the vacuum system. Turn on the vacuum pump (13) and adjust the regulating valve to achieve the preselected ultimate chamber pressure.

3. Adjust the three-way valve to isolate the drying chamber from the vacuum system. Move the sample mold (5) from the freezer (16) quickly into the drying chamber after weighing, and cover the bell jar and reconnect the drying chamber to the vacuum system.

4. Start the data acquisition system recording variations of the sample weight, W_t, the ambient temperature and the ambient pressure with time.

5. Observe the mass variation with time until there is no significant change displayed on the computer screen.

6. Stop the data acquisition system. Switch off the vacuum pump and adjust the three-way valve for venting.

7. Turn off the circulator and the blower. Remove the dried product from the chamber and measure its residual

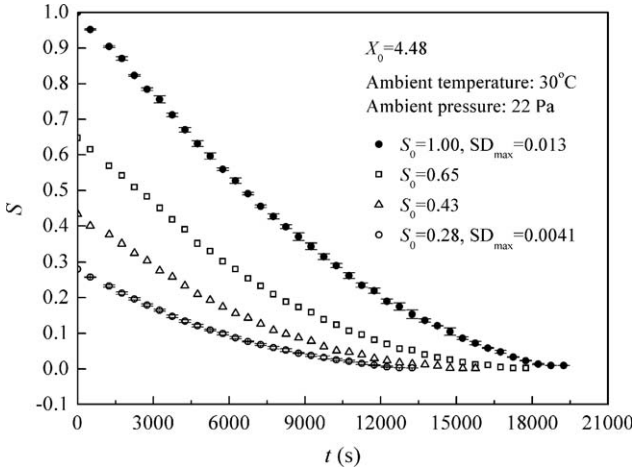

Figure 3. Freeze-drying curves of samples with different initial saturations.

moisture content using the drying cabinet and the moisture analyzer, respectively.

The dry-based moisture content of the sample during drying is

$$X_t = \frac{W_t - W_s}{W_s} \tag{4}$$

where W_s (kg) is the solid mass of the sample obtained from Eq. 1. The moisture content can also be expressed in terms of ice saturation using the following formula

$$S = \frac{(1-\varepsilon)\rho_s}{\varepsilon \rho_i} \cdot X_t \tag{5}$$

As freeze-drying was normally operated below 50°C of temperature and in the range of 4–40 Pa of pressure,[7,31] 30°C of the ambient temperature and 22 Pa of the ambient pressure were selected as the typical operating conditions in the present tests. The experimental data were acquired at a frequency of 0.5 Hz, which was sufficient to obtain a reliable data set for the drying process. To smooth out electronic noise, the data were averaged arithmetically over a certain time period to generate each data point. Because plenty of data were collected, the subsequent drying figures only display those within about 500 s of a time interval.

Results and Discussion

Effect of initially unsaturated materials on freeze-drying

By keeping the same sample mass, the same initial moisture content and also the same drying conditions, the experimentally measured drying curves are shown in Figure 3. It is worth noting that triplicate tests were conducted for the saturated frozen samples and the unsaturated ones with 0.28 of the initial saturation to quantify the repeatability of the experimental data. The results all demonstrated excellent reproducibility with 0.013 and 0.0041 of the maximum standard deviation of all data points on their respective drying curves as plotted in Figure 3. Replicate tests were conducted for the other two cases of different initial saturations. Excellent agreements were also achieved for each pair of the drying curves. All the data presented in Figure 3 are the average values of the replicate or triplicate tests. It is expected to find that the smaller the initial saturation of frozen materials, the shorter the drying time. The initially unsaturated frozen material can indeed enhance the freeze-drying of liquid materials, and the proposed technique can be feasible and quite effective. The greatest improvement clearly occurred for the sample with S_0 being 0.28 taking 12,750 s of drying time compared with 18,750 s for its saturated counterpart, indicating 32% beneficial effect under the current operating conditions. With the sample configuration tested, sublimated vapor would migrate along both the axial and radial directions during drying. Because of the same radius, the sample with smaller initial saturation was taller. The taller the cylindrical sample, the larger the share of mass transfer in the radial direction.

Meanwhile, there was no collapse of the structure judged from the drying curves, and no crack or deformation from the dried products appeared during and after freeze-drying as seen in the next section.

It is interesting to note in Figure 3 that besides the shorter drying time, the sample of smaller initial saturation had lower residual moisture content in the dried product. Table 2 lists the drying times and the average values of the wet-based residual moisture contents of the different products. The frozen material with smaller initial saturation had a larger pore size for sublimated vapor to pass through. Meanwhile, the smaller initial saturation also produced a more tenuous solid matrix, which promotes desorption of bound moisture, resulting in a lower moisture content in the dried product.

Figure 4 shows normalized drying rate curves for the four samples with different initial saturations based on the data shown in Figure 3. For the sake of convenient analysis, the relative saturation, f, defined as the ratio of the real-time saturation to the initial saturation (S/S_0), is used in the presentation. In the early stage of drying, the drying rate of the initially unsaturated samples was obviously higher than that of the saturated one, and the smaller the initial saturation, the faster the drying rate. In the latter stage of drying, when the residual moisture content was already low (around $f = 0.1$), the drying rates dropped rapidly, and the differences among the drying rates for the samples with different initial saturations was no longer significant. In the end of drying, the superiority of small mass-transfer resistance by the initially unsaturated materials was insignificant, and heat transfer consequently became the major rate-controlling factor in the process for all cases.

It can be estimated that for the initially unsaturated frozen material with the same sample mass and the same initial moisture content, lower initial saturation gave a larger internal surface area in the porous matrix. The moisture would exist largely in the form of the bound moisture absorbed in the internal surface, and the share of the free moisture would be correspondingly lower for this type of the frozen material. The freezing-drying mechanism for the unsaturated frozen material is, therefore, likely to be different from that of the

Table 2. Drying Times and Residual Moisture Contents of Different Samples

S_0	Drying Time (s)	Residual Moisture Content (%)
1.00	18,750	4.01
0.65	17,250	2.29
0.43	15,250	1.83
0.28	12,750	0.61

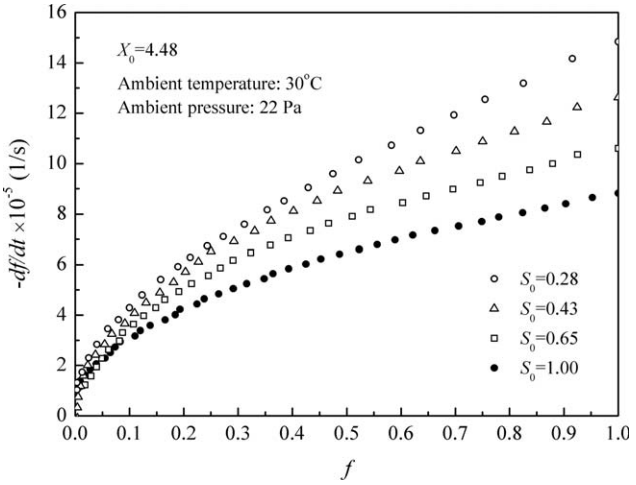

Figure 4. Drying rate curves of samples with different initial saturations.

saturated one. Most probably, the primary drying time can be saved due to the initially prebuilt pore space and the relatively large surface area inside the material. The overall result is that the freeze-drying of aqueous solutions can be significantly enhanced using the unsaturated frozen material with initial pores.

Morphological characterization of freeze-dried products

To inspect the pore structure and the connectivity of the dried solid matrixes, two kinds of the dried products from the initially saturated ($S_0 = 1.00$) and unsaturated ($S_0 = 0.28$) frozen samples were characterized with a scanning electronic microscope (SEM). The SEM allows direct observation of the surface features of a specimen in contrast with indirect methods such as adsorption and mercury porosimetry, due to its huge magnifications and impressive resolutions at the micron and submicron levels.[32] It has been widely used in many areas of science and industry, particularly in the material engineering and the biological and medical sciences. The SEM process is briefly described as follows. A specimen of the dried product was first mounted onto a specimen stub and then sputter-coated with an ultrathin layer of gold to give it electrical conductivity. Afterwards, it was inserted to the stub holder within the SEM chamber for scanning and imaging at 20 kV of voltage, 4.0 of spot size, and either 16.8 or 18.8 mm of working distance. Figure 5 shows some of the SEM images, in which Figures 5a–c are for the freeze-dried product obtained from the saturated frozen sample and Figures 5d–f are for the product from the initially unsaturated one.

The morphology as seen in Figure 5a typically exhibits a platelet-shaped structure where the platelet edges appear in white and light gray colors and pore areas in dark gray color. This is consistent with the previously published observation.[33] It is well accepted that solutions would experience a cool concentration during freezing. The solid phase probably precipitated first because the mannitol reached its solubility limit. As the solution was cooled further, more liquid water converted into ice and remaining interstitial fluid became more and more concentrated until crystallizing or

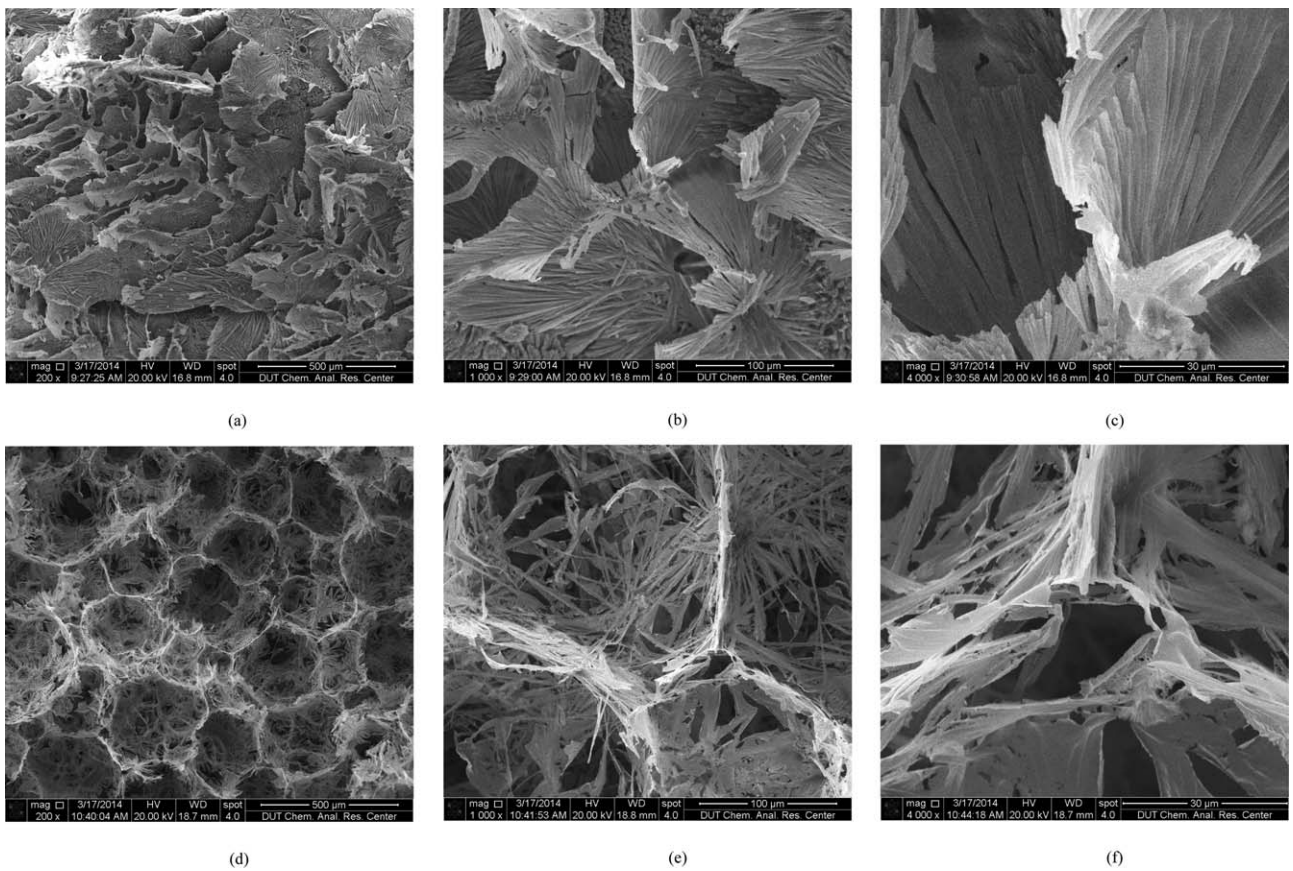

Figure 5. SEM images of dried products with two freezing methods at different magnifications; (a)–(c) for the initially saturated sample; (d)–(f) for the initially unsaturated one.

transforming into an amorphous solid ultimately.[31] The growth of ice crystals pushed the solid in their vicinity into a sheet structure. However, careful observation of Figures 5b, c reveals that the solid skeleton is composed of crystalline bars adhering to each other. Although the interstitial fluid in this case solidified in the crystalline form, the skeleton walls look more compact and almost closed. It is conceivable from Figures 5a–c that the shape of the ice crystals is irregular, which agrees well with results obtained using the optical microscopy.[34]

The morphology of the dried skeleton from the initially unsaturated sample is dramatically different from that of the saturated one. A notable feature of Figures 5d–f is that the freeze-dried product appears to have a fine net structure that is loose and regular. The compacting of the dried solids into the skeleton is not as tight as that for the conventionally freeze-dried product, and the skeleton remains much more porous after drying. It is with this new freezing method that such a solid structure was eventually established. For this type of frozen materials, ice crystals have more room to grow in the prebuilt pores during freezing. As a result, there was no deformation induced by expansion found during further freezing at an ultralow temperature. It is seen in Figures 5d, e that the solid skeleton with the new method is more tenuous and uniform than that with the conventional method. More importantly, the unsaturated frozen material made by the liquid nitrogen ice-cream making method has continuous pore space and pierced solid skeleton. It is also seen in Figures 5e, f that the skeleton is composed of slender crystalline belts, looking like a mesh and allowing vapor molecules to pass through. Such a loose structure would offer less mass-transfer resistance so that sublimated vapor could escape more easily during drying, leading to a higher drying rate. That is most likely the reason why freeze-drying time can be saved with this freezing protocol and the process can be enhanced using the frozen material with initial pores.

It should be pointed out that the surface morphologies reveal no clear evidence of collapse for both kinds of the products. Furthermore, a computer image analysis of the SEM images was performed using ImageJ—a Java-based software to evaluate the area porosity of the dried products.[35] Area-based porosities of 0.87 and 0.96 were obtained for the products from the initially saturated and unsaturated samples, respectively. The two values compare well with the volume-based experimental measurements as shown in Table 1.

Temperature variations at different locations within materials

Figure 6 displays the temperature variations recorded at different locations within the two kinds of sample as used in the above subsection, where the filled markers represent the saturated frozen sample and the open markers the initially unsaturated one. Test points 1, 2, and 3 are indicated in Figure 2. At the very beginning of drying, there was a sudden drop in temperature for both samples. This is the consequence of the dynamic balance between the heat and mass transfers. The stable temperature after the initial drop would establish when the heat-transfer driving force supplies the heat required for the subsequent sublimation of the ice.

The temperatures at points 1, 2, and 3 in the initially saturated sample gradually increased after the sudden drop until about 8,000 s, and then slowly decreased before increasing again. For such a sample without initial pores, sublimation is

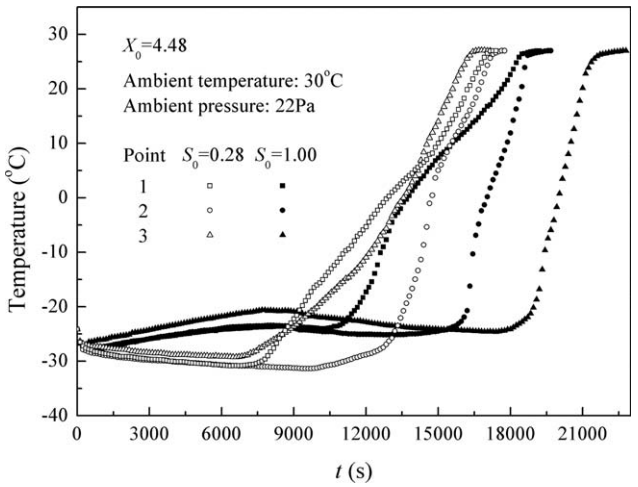

Figure 6. Temperature variations of two different samples during drying.

known to occur only at the sublimation interface.[11] In the early stage of drying before 8,000 s, heat transported from the surroundings was more than needed due to the relatively low sublimation intensity. Excess heat absorbed caused a slight increase in the sample temperature. With the progressing of the drying process, a porous semidried layer with a certain thickness gradually developed which hindered heat transfer between the sample and the surroundings. To maintain a similar sublimation rate at the interface, a slightly large temperature driving force was required resulting in a slightly reduced temperature at the interface. The temperature at point 1 began to increase fast after about 10,500 s. This implies the end of the primary drying stage and the start of the secondary drying stage.[36,37] As point 1 is closer to the side surface of the sample, the sublimation interface receded to that location first. Points 2 and 3 entered the desorption drying stage at about 15,000 and 18,000 s, respectively. Comparison of the temperatures between points 1 and 2 reveals that they were almost the same within the initial 10,000 s of drying. Afterwards, the two points started experiencing desorption successively. This indicates that there was an evident sublimation interface existing in the conventional freeze-drying of the initially saturated frozen material. Comparison of point 2 with point 3 shows that the temperature at point 3 was higher than that of point 2 at the sublimation drying stage. This can be explained by heat conduction from the supporting pad resulting in an axial temperature gradient because point 3 is closer to the supporting pad. Although the temperature at point 3 was higher than that of point 2, the sublimation interface reached point 3 later. This implies that there was a frozen region always within the sample at the sublimation drying stage, and sublimated vapor could not pass through that region moving out of the sample. Therefore, except at the very beginning, the predominant rate-controlling factor for the initially saturated frozen material is mass transfer during the long period after a dried layer had formed. This is consistent with previously published findings.[19,20] In the end of drying, the temperatures at all three points had almost the same values at about 27°C.

For the initially unsaturated sample, the temperature variations at all three points were different from those of the saturated one. The three temperatures slowly decreased

throughout the primary drying stage due to the relatively high sublimation rate. In contrast to the saturated sample as stated earlier, heat-transfer resistance for this sample on average was greater than that of the saturated one due to the prebuilt porous structure. Because of the higher sublimation rate than that of the saturated one, a larger temperature driving force was required for this case leading to the continuously decreased temperature noticed in this stage of drying. As the unsaturated sample had the initially prebuilt void space and a pierced solid matrix, sublimation could take place throughout the entire volume of the sample. Both points 1 and 2 had the similar temperatures at the primary drying stage and started desorption at about 7,500 and 11,000 s in sequence. This indicates that there was still a main sublimation region during freeze-drying of the initially unsaturated material. The transition time between the two stages at point 3 was about 7,000 s, which is very close to that at point 1. The large initial pore space in the unsaturated frozen material offered less mass-transfer resistance and ice crystals throughout the frozen region could sublimate simultaneously. Different from the saturated sample, the main sublimation region went to point 3 earlier at the primary drying stage for this type of the material because of heat transfer from the pad, which also explains the slightly higher temperature documented at point 3 with both samples. The delayed onset of the secondary drying stage at point 2 in the center of the sample is understandable because of less heat absorbed from the outside in and long distance migration of sublimated vapor moved from the inside out. It is impressive to observe that the three points reached the end of drying almost simultaneously in this sample. This again demonstrates that sublimation was proceeding throughout the entire volume of the material, although at different rates.

Further observation on temperature evolutions of the two samples reveals that the initially unsaturated sample spent less time at the primary drying stage. This suggests that the enhanced freeze-drying performance for the initially unsaturated material arises mainly from the enhanced sublimation during the primary drying stage, where the free moisture is removed more quickly. However, the drying time at the secondary drying stage was very similar for both samples. This implies that the removal of the bound moisture during the secondary drying stage is also promoted because of the large internal surface area, although the share of the bound moisture is increased in this type of the material as stated previously. Compared with the conventional freeze-drying where the predominant rate-controlling factor is mass transfer as reviewed earlier,[19–24] freeze-drying of the initially unsaturated material is mainly controlled by heat transfer. As a result, the enhanced heat transfer from a moderately high driving force is expected to decrease the freeze-drying time further for the initially unsaturated frozen material.

Effects of operating conditions

Ambient temperature and pressure are considered to be the two important parameters affecting the freeze-drying process. As the pore structure of the initially unsaturated frozen material is different from that of the conventional one as discussed earlier, the effects of the operating conditions on the process might be expected to be different. Consequently, these two parameters were examined in more details. It has to be pointed out that no replicate tests were conducted for this part of experiments because of the excellent repeatability of the experimental data proven previously.

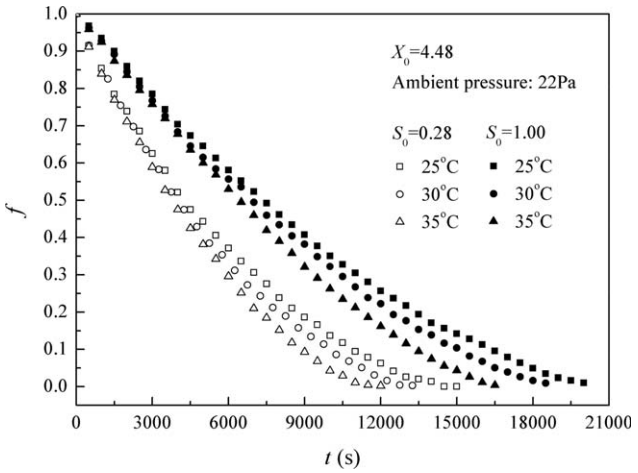

Figure 7. Drying curves of two different samples at three ambient temperatures.

The effect of temperature was examined using two samples with the initial saturations of 1 and 0.28. The experiments were carried out at a constant ambient pressure of 22 Pa and three ambient temperatures of 25, 30, and 35°C. The drying curves are shown in Figure 7.

It is seen that the drying times for both samples decreased with the increase in temperature. When the ambient temperature increased from 25 to 35°C under the present operating conditions, about 18% of the drying time was saved for both samples. Although the appropriate increase in ambient temperature is accepted as one of the effective approaches to the enhancement of the freeze-drying process as demonstrated by vial freeze-drying experiments,[9] excessively high ambient temperature could cause melting of the frozen materials or collapse of the solid structure, which would ruin the overall freeze-drying process. Comparing each pair of the drying curves of both samples under the same operating conditions, it is clear in Figure 7 that the initially unsaturated samples ($S_0 = 0.28$) were dried much faster than the saturated ones ($S_0 = 1.00$). This is consistent with those found in Figure 3, and increasing drying temperature can surely boost the drying rate as expected.

Similar samples were used to examine the effect of the chamber pressure on the freeze-drying process. Three ambient pressures of 11, 22, and 33 Pa were used in these experiments with a constant ambient temperature of 30°C. The drying curves are shown in Figure 8. It is also seen from the drying curves in Figure 8 that the beneficial effect of using the initially unsaturated frozen material was very significant. The ambient pressure, however, had little effect on the freeze-drying performance for the conventional sample. This was the result of the two opposite effects caused by the pressure variation. On the one hand, the decrease in pressure is well accepted to improve the effective mass diffusivity, which is conducive to mass transfer for a freeze-drying process. Conversely, the ultralow ambient pressure decreases the effective thermal conductivity, which impairs heat transfer. In the vial freeze-drying process, Brulls and Rasmuson pointed out that the possible modes of heat exchange are heat conduction through the gas between the vial and the surroundings, thermal radiation and heat conduction by

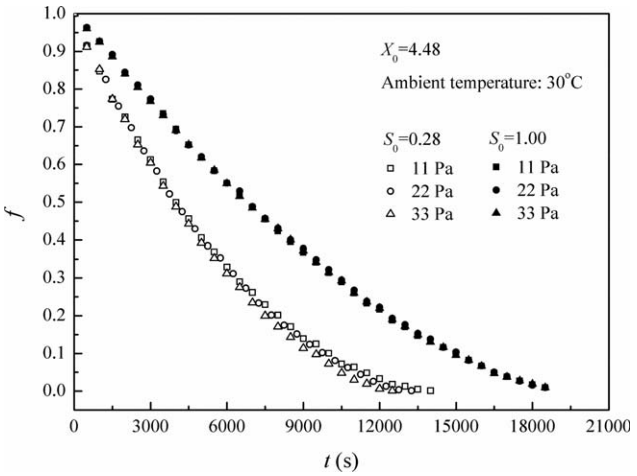

Figure 8. Drying curves of two different samples at three ambient pressures.

direct contact between the shelf and the vial. They concluded that the overall heat-transfer coefficient increases proportionally with increasing chamber pressure.[38] Pikal and coworkers found that under relatively low chamber pressure, the increase in pressure can be significantly helpful for heat transfer, but useless for mass transfer.[9] Nail observed that increasing chamber pressure can result in an increase in the primary drying rate.[39] Because of no container or vial in these experiments, the improvement of heat conduction by gas contact was not sensitive to the pressure in comparison with the samples in vial. The effects of the ambient pressure on both mass transfer and heat transfer apparently counteracted each other for the conventional sample.

Careful observation of Figure 8 reveals only an insignificantly small decrease with pressure in the drying time for the initially unsaturated frozen sample. This can be explained by the larger prebuilt pores, where vapor transport resistance is accordingly small. The effect of higher pressures on the effective heat conductivity may be slightly beneficial. In comparison with the effect of the ambient temperature on this type of the material, the effect of the ambient pressure can be neglected.

Conclusions

An initially unsaturated frozen material can be made by mixing liquid nitrogen with the aqueous solution to be freeze-dried. The initially unsaturated frozen material has larger internal surface area, much thinner solid network, and more uniform continuous pore space than the initially saturated frozen material. This morphology is quite helpful for increasing sublimation–desorption surface area, facilitating vapor migration, thus reducing the mass-transfer resistance and improving the freeze-drying rate.

The experimental results show that the freeze-drying of liquid materials can be significantly enhanced by inducing initial pores in the frozen material. The freeze-drying time was found to decrease with the increase in initial porosity. For two samples with the same initial mass and the same initial moisture content, the drying time of the initially unsaturated frozen sample ($S_0 = 0.28$) was 32% shorter than that of the initially saturated one ($S_0 = 1.00$) under the same operating conditions. Examination of temperature variations inside the two kinds of samples during drying reveals that the initially unsaturated frozen material has much more beneficial effect on the free moisture removal at the primary drying stage. Sublimation for this type of the material takes place at the internal surface throughout the entire volume. This prebuilt porous structure with larger internal surface area also promotes the bound moisture removal at the secondary drying stage. The increase in ambient temperature can further enhance the drying rate while the change in ambient pressure has insignificant effect.

The idea of using the prebuilt porous frozen material is easy to implement and highly effective in improving the freeze-drying performance. Future freeze-drying of high value products from aqueous solution can benefit from this process.

Acknowledgments

The authors highly appreciate the financial supports from the Fundamental Research Funds for the Central Universities (DUT14RC(3)008), the National Natural Science Foundation of China (NNSF21076042) and the Research Grants Council of Hong Kong SAR (HKUST600704).

Literature Cited

1. Choi MJ, Briancon S, Andrieu J, Min SG, Fessi H. Effect of freeze drying process conditions on the stability of nanoparticles. *Drying Technol*. 2004;22:335–346.
2. Sadikoglu H, Ozdemir M, Seker M. Freeze-drying of pharmaceutical products: research and development needs. *Drying Technol*. 2006;24:849–861.
3. Wang W, Chen G, Mujumdar AS. Physical interpretation of solids drying: an overview on mathematical modeling research. *Drying Technol*. 2007;25:659–668.
4. Sun X, Peng B, Ji Y, Chen J, Li D. Chitosan (chitin)/cellulose composite biosorbents prepared using ionic liquid for heavy metal ions adsorption. *AIChE J*. 2009;55:2062–2069.
5. Schwegman JJ, Hardwick LM, Akers MJ. Practical formulation and process development of freeze-dried products. *Pharm Dev Technol*. 2005;10:151–173.
6. Wang W, Chen M, Chen G. Issues in freeze drying of aqueous solutions. *Chin J Chem Eng*. 2012;20;551–559.
7. Nail SL, Jiang S, Chongprasert S, Knopp SA. Fundamentals of freeze-drying. In: Nail SL, Akers MJ, editors. *Development and Manufacture of Protein Pharmaceuticals*. New York: Kluwer Academic/Plenum Publishers, 2002:281–361.
8. Wang W, Chen G. Theoretical study on microwave freeze-drying of an aqueous pharmaceutical excipient with the aid of dielectric material. *Drying Technol*. 2005;23:2147–2168.
9. Pikal MJ, Roy ML, Shah S. Mass and heat transfer in vial freeze-drying of pharmaceuticals: role of the vial. *J Pharm Sci*. 1984;73:1224–1237.
10. Liapis AI, Pikal MJ, Bruttini R. Research and development needs and opportunities in freeze drying. *Drying Technol*. 1996;14:1265–1300.
11. Liapis AI, Bruttini R. Freeze drying. In: Mujumdar AS, editor. *Handbook of Industrial Drying*, 2nd ed., Vol. 2. New York: Marcel Dekker, 1995:305–343.
12. Wang W, Chen G. Numerical investigation on dielectric material assisted microwave freeze-drying of aqueous mannitol solution. *Drying Technol*. 2003;21:995–1017.
13. Wang W, Chen G. Freeze drying with dielectric-material-assisted microwave heating, *AIChE J*. 2007;53:3077–3088.
14. Ratti C. Hot air and freeze-drying of high value foods: a review, *J Food Eng*. 2001;49:311–319.
15. Song CS, Nam JH. An efficient calculation of multidimensional freeze-drying problems using fixed grid method. *Drying Technol*. 2005;23:2491–2511.
16. Sheehan P, Liapis AI. Modeling of the primary and secondary drying stages of the freeze drying of pharmaceutical products in vials: numerical results obtained from the solution of a dynamic and spatially multi-dimensional lyophilization model for different operational policies. *Biotechnol Bioeng*. 1998;60:712–728.

17. Wang ZH, Shi MH. The effects of sublimation-condensation region on heat and mass transfer during microwave freeze drying. *J Heat Trans-T ASME*. 1998;120:654–660.
18. Chen M, Wang W, Pan YQ, Yu K, Chen G. 1D and 2D numerical verification on freeze drying of initially porous material frozen from aqueous solution. In: Chen XD, Mujumdar AS, editors. CD-ROM Proceedings of 18th International Drying Symposium (IDS2012). Xiamen, China: XMU, 2012:11.
19. Livesey RG, Rowe TW. A discussion of the effect of chamber pressure on heat and mass transfer in freeze-drying. *J Parenter Sci Technol*. 1987;41:169–171.
20. Wolff E, Gibert H, Rodolphe F. Vacuum freeze-drying kinetics and modeling of a liquid in a vial. *Chem Eng Process*. 1989;25:153–158.
21. Nail SL, Gatlin LA. Freeze drying: principle and practice. In: Avis A, Liebermann A, Lachmann L, editors. *Pharmaceutical Dosage Forms*, Vol. 2. New York: Marcel Dekker, 1993:163–333.
22. Nakagawa K, Hottot A, Vessot S, Andrieu J. Modeling of freezing step during freeze-drying of drugs in vials. *AIChE J*. 2007;53:1362–1372.
23. Wang W, Chen G. Heat and mass transfer model of dielectric-material-assisted microwave freeze-drying of skim milk with hygroscopic effect. *Chem Eng Sci*. 2005;60:6542–6550.
24. Pikal MJ, Shah S, Senior D, Lang JE. Physical chemistry of freeze-drying: measurement of sublimation rates for frozen aqueous solutions by a microbalance technique. *J Pharm Sci*. 1983;72:635–650.
25. Wang W. Dielectric-material-assisted microwave freeze-drying of aqueous solution, Ph.D. Dissertation. Hong Kong University of Science and Technology, Hong Kong, 2005.
26. Yu K, Wang W, Pan Y, Wang W, Chen G. Effect of initially unsaturated porous frozen material on freeze-drying. *CIESC J*. 2013;64:3110–3116.
27. Tang XL, Pikal MJ. Design of freeze-drying processes for pharmaceuticals: practical advice. *Pharm Res*. 2004;21:191–200.
28. Bam NB, Randolph TW, Cleland JL. Stability of protein formulations: investigation of surfactant effects by a novel EPR spectroscopic technique. *Pharm Res*. 1995;12:2–11.
29. Hartel RW. Phase transitions in ice cream. In: Rao MA, Hartel RW, editors. *Phase/State Transitions in Foods*. New York: Marcel Dekker, 1998:327–331.
30. Donhowe DP, Hartel RW, Brakley RL. Determination of ice crystal size distribution in frozen desserts. *J Dairy Sci*. 1991;74:3334–3344.
31. Pikal MJ. Freeze drying. In: Swarbrick J, editor. Encyclopedia of Pharmaceutical Technology. New York: Marcel Dekker, 2002:1299–1326.
32. Daley MA, Tandon D, Economy J, Hippo EJ. Elucidating the porous structure of activated carbon fibers using direct and indirect methods. *Carbon*. 1996;34:1191–1200.
33. Hawe A, Friess W. Physico-chemical lyophilization behavior of mannitol, human serum albumin formulations. *Eur J Pharm Sci*. 2006;28:224–232.
34. Nakagawa K, Hottot A, Vessot S, Andrieu J. Influence of controlled nucleation by ultrasounds on ice morphology of frozen formulations for pharmaceutical proteins freeze-drying. *Chem Eng Process*. 2006;45:783–791.
35. Choudhari KS, Jidesh P, Sudheendra P, Kulkarni, SD. Quantification and morphology studies of nanoporous alumina membranes: a new algorithm for digital image processing. *Microsc Microanal*. 2013;19:1061–1072.
36. Pikal MJ, Shah S, Roy ML, Putman R. The secondary drying stage of freeze drying: drying kinetics as a function of temperature and chamber pressure. *Int J Pharmaceut*. 1990;60:203–217.
37. Liapis AI, Bruttini R. A theory for the primary and secondary drying stages of the freeze-drying of pharmaceutical crystalline and amorphous solutes: comparison between experimental data and theory. *Sep Tech*. 1994;4:144–155.
38. Brulls M, Rasmuson A. Heat transfer in vial lyophilization. *Int J Pharmaceut*. 2002;246:1–16.
39. Nail SL, The effect of chamber pressure on heat transfer in the freeze drying of parenteral solutions. *J Parenter Drug Assoc*. 1980;34:358–368.

Manuscript received Aug. 15, 2014, and revision received Dec. 31, 2014.